Hydraulic Design of a USBR Type II Stilling Basin

Roberta Padulano, Ph.D.[1]; Oreste Fecarotta[2]; Giuseppe Del Giudice, M.ASCE[3]; and Armando Carravetta[4]

Abstract: The present paper deals with a United States Bureau of Reclamation (USBR) Type II stilling basin, which is characterized by blocks at the end of the chute and a dentated sill at the end of the basin. For this basin, USBR only gives overall design criteria concerning basin length and block dimensions on the basis of the assumption that the hydraulic jump remains confined within the sill. No considerations are provided concerning possible different jump types, pressure regimes, and forces acting on the sill. To comply with such a lack, an experimental campaign was undertaken that focuses on the differences among hydraulic jump types that can occur in a USBR Type II stilling basin. Jump types can range between submerged and spray jump types; accordingly, dimensionless relations are provided to predict jump type and position for assigned boundary conditions, with particular concern about the submerged/nonsubmerged distinction. Considerations about the drag force and drag coefficients are provided, along with estimates of pressure extreme fluctuations. Finally, an evaluation of the dissipation efficiency is presented for both submerged and nonsubmerged jumps, enabling comparisons among different jump types and with classical hydraulic jump. **DOI: 10.1061/(ASCE)IR.1943-4774.0001150.** © *2017 American Society of Civil Engineers.*

Author keywords: Dissipation efficiency; Drag coefficient; Hydraulic jump; Jump types; USBR Type II stilling basin.

Introduction

Stilling basins are required in storage and detention dams to reduce the excess kinetic energy of the water flowing downstream by means of a turbulent vortex structure induced by the hydraulic jump (Alikhani et al. 2010; Tiwari and Goel 2014; Chanson 2015). Various types of stilling basins are United States Bureau of Reclamation (USBR) stilling basins (Bradley and Peterka 1957), manifold stilling basins (Fiala and Albertson 1961), Contra Costa energy dissipators (Keim 1962), Utah State University (USU) energy dissipators (Flammer et al. 1970), counter current energy dissipators (Vollmer and Khader 1971), Verma energy dissipators (Verma and Goel 2000), and Mahakaal stilling basins (Tiwari et al. 2011) among others. Vischer and Hager (1999) recommend that this type of structure is designed economically in terms of length, tailwater level, scour, and cavitation.

In this paper, data stemming from the experimental campaign performed on the 1:70 physical model of the Lower Diamphwe Dam (Malawi), described in Fecarotta et al. (2016), are analyzed. The dam is equipped with an uncontrolled spillway and a USBR Type II stilling basin (Bradley and Peterka 1957), which is provided with blocks at the end of the chute and a dentated sill at the end of the basin (Fig. 1). The aim of this paper is the study of its hydraulic behavior. USBR only gives overall design criteria concerning basin length and block dimensions; such considerations are on the basis of the assumption that the hydraulic jump remains confined within the sill, whereas no considerations are provided concerning possible different jump types, pressure regimes, and forces acting on the sill. Conversely, in-depth studies are available concerning different types of stilling basins (Ohtsu et al. 1991; Hager and Li 1992). This paper focuses on the differences among hydraulic jump types that can occur in such a basin, providing dimensionless relations to predict jump type and position. Moreover, measurements of pressure fluctuation upstream and downstream of the dentated sill were performed and pressure fluctuations were related to the dissipation efficiency of the dentated sill. Finally, considerations about the drag force acting on the sill are provided for a correct design of the basin.

Review of Literature

The influence of the geometry of a stilling basin on the hydraulic characteristics of the flow has been studied by several researchers. Ohtsu et al. (1991) and Hager and Li (1992) described the effect of a continuous end sill on the hydraulic jump, whereas Habibzadeh et al. (2011) studied the dissipation efficiency of baffle blocks when a submerged jump occurs. Moreover, Peterka (1984) offered criteria for a correct preliminary design of confining elements (chute, dentated sill, and basin length) on the basis of a number of already existing Type II basins and experimental tests, provided that the operating conditions cause a hydraulic jump that is completely confined within the basin. However, no systematic experimental investigation is available concerning a Type II stilling basin; therefore, the state-of-the-art only provides for a general understanding about hydraulic behavior of stilling basins and design of experiments.

Sequent Depths

All of the examined papers relied on classical hydraulic jump (CHJ) variables (hydraulic jumps induced or constrained by some

[1]Dept. of Civil, Architectural and Environmental Engineering, Università degli Studi di Napoli Federico II, 80125 Napoli, Italy (corresponding author). E-mail: roberta.padulano@unina.it

[2]Assistant Professor, Dept. of Civil, Architectural and Environmental Engineering, Università degli Studi di Napoli Federico II, 80125 Napoli, Italy. E-mail: oreste.fecarotta@unina.it

[3]Associate Professor, Dept. of Civil, Architectural and Environmental Engineering, Università degli Studi di Napoli Federico II, 80125 Napoli, Italy. E-mail: delgiudi@unina.it

[4]Associate Professor, Dept. of Civil, Architectural and Environmental Engineering, Università degli Studi di Napoli Federico II, 80125 Napoli, Italy. E-mail: arcarrav@unina.it

Note. This manuscript was submitted on April 21, 2016; approved on September 21, 2016; published online on January 18, 2017. Discussion period open until June 18, 2017; separate discussions must be submitted for individual papers. This paper is part of the ***Journal of Irrigation and Drainage Engineering***, © ASCE, ISSN 0733-9437.

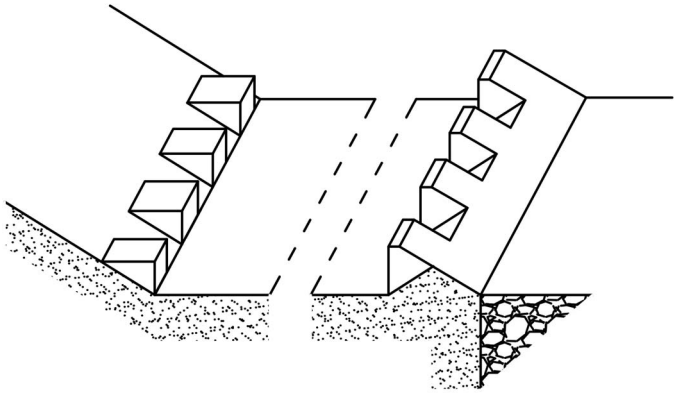

Fig. 1. USBR Type II stilling basin

kind of appurtenances are referred to as "forced" as opposed to CHJ) to describe the hydraulic behavior of confined stilling basins. For a given discharge, Q, approaching a rectangular channel in which a CHJ occurs, h_1 is the water depth at the jump toe and F_1 is the corresponding Froude number in supercritical flow ($\mathsf{F}_1 = V_1/\sqrt{gh_1}$ in which V_1 is the approach flow velocity and g is the acceleration because of gravity). For a CHJ, h_2^* is usually denoted as the subcritical sequent depth, and the sequent depth ratio h_2^*/h_1 is

$$\frac{h_2^*}{h_1} = [(1 + 8\cdot)^{1/2} - 1] \tag{1}$$

known as the Belanger equation (Chow 1959).

In real applications, the subcritical flow depth is fixed by a downstream control to a value h_t (tailwater depth), which generally is different from h_2^*. This implies that the hydraulic jump shifts downstream (if $h_t < h_2^*$) or upstream (if $h_t > h_2^*$), and Eq. (1) must be recomputed; for this reason, the tailwater depth-discharge relation must be carefully known (Vischer and Hager 1999). If $h_t \gg h_2^*$, the hydraulic jump may have no room to develop (submerged jump); the water profile is roughly horizontal and turbulence develops below the free surface. If $h_t \ll h_2^*$, the hydraulic jump could be swept out of the basin, causing excessive scour of the river bed. The latter condition usually is considered inacceptable (Habibzadeh et al. 2011), whereas submerged jumps often are allowed, although in this case, the dissipation efficiency was lower than nonsubmerged jumps because of the poor jet mixing. In some cases, however, submerged jumps are preferred because they are less sensitive to tailwater variations.

Jump Types and Depth of Incipient Submergence

In a forced jump (either submerged or nonsubmerged), all the CHJ characteristic relations must be recomputed to account for the influence of the specific appurtenance limiting the basin, which could be, for instance, a continuous vertical or sloping sill or alternate blocks (Hager 1992). In such cases, an additional variable must be accounted for, namely $L_s = L_B - x_p$, if L_B and x_p are the positions of the appurtenance and of the jump toe from a fixed point, respectively. Conventionally, $x_p = 0$ implies the jump toe position coincides with the end of a chute or with the sluice gate causing the supercritical flow, whereas $x_p < 0$ implies a submerged jump. This conventional notation will be assumed in the present paper, with the fixed reference point set at the terminal section of the chute. For decreasing L_s, different types of hydraulic jumps can be observed, as described in the following by Hager and Li (1992) for sill-controlled basins (Fig. 2):

- Submerged jump;
- A-jump, with end of the roller before or over the confining appurtenance;
- B-jump, with the roller extending beyond the appurtenance with a small standing wave;
- Minimum B-jump (B_m), same as B-jump, but with a definite second surface roller downstream of the appurtenance;
- C-jump, with a downstream standing wave involving considerable pulsation and development of spray; and
- Spray or wave type jump with supercritical flow over the appurtenance and unacceptable energy dissipation.

For a fixed approach Froude number, jump type evolves from submerged to spray for decreasing tailwater with a fixed sill height, or for increasing sill height, with a fixed tailwater level. For fixed L_B and sill height D, a particular tailwater h_2^A (depth of incipient submergence) can be defined so that the forced jump is submerged if $h_t > h_2^A$; in other words, h_2^A is the sequent depth of h_1 for forced A-jumps, and it is always $h_2^A < h_2^*$. This means that the appurtenance enables control and stabilization of the jump position for a lower tailwater than free jumps (Hager 1992).

For sill-controlled nonsubmerged jumps, Hager and Li (1992) provided a dimensionless abacus to predict jump type (or jump position) for given incoming Froude number, tailwater depth, sill height, and position. Such an abacus stems from the consideration that the sequent depth ratio h_t/h_1 for forced jumps can be obtained by subtracting the effect of the sill ΔY_s from the CHJ sequent depth ratio, once the effect of wall friction is neglected

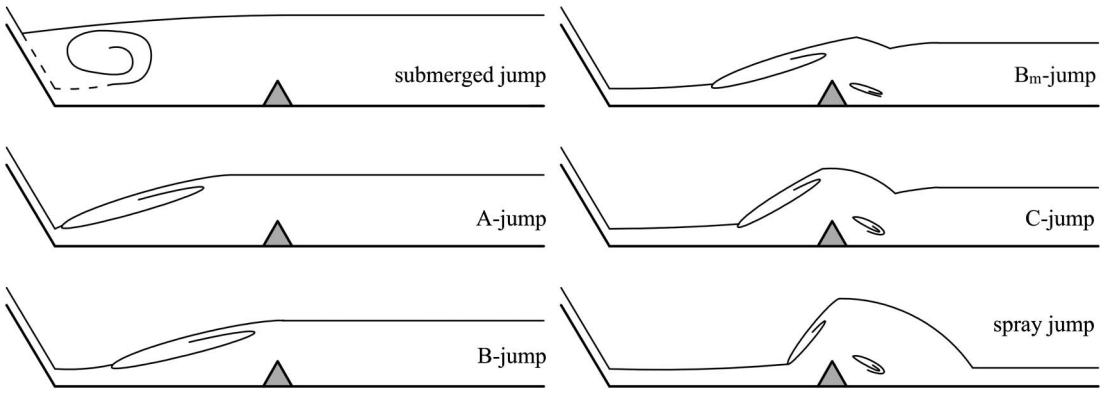

Fig. 2. Jump types as described by Hager and Li (1992)

$$\frac{h_t}{h_1} = \frac{h_2^*}{h_1} - \Delta Y_s \tag{2}$$

The effect of the sill depends on both the jump position and the sill height. Dimensionless variables adopted by Hager and Li (1992) to describe ΔY_s are $1 - L_s/L_j^*$ and D/h_1; L_j^* is the length of CHJ and can be computed by means of different relations as suggested by Hager (1992). Specifically, ΔY_s increases for increasing sill height and decreasing distance between jump toe and sill.

Dissipation Efficiency

For confined basins, the energy dissipation consists in the energy loss, namely the difference between the specific energies before and after the jump; the dissipation efficiency is defined as the ratio of the energy dissipation to the specific energy before the jump. For submerged jumps with baffle blocks, Habibzadeh et al. (2011) found that the dissipation efficiency has a maximum for low submergence factors $S = (h_t - h_2^*)/h_2^*$, whereas it increases with increasing F_1 for fixed S. Also, efficiency is greater for slightly submerged jumps with blocks than for nonsubmerged jumps with blocks, whose efficiency is, in turn, greater than the efficiency of a CHJ (Govinda Rao and Rajaratnam 1963). However, dissipation efficiency for a basin with a continuous sill generally is greater than the efficiency of a basin with baffle blocks because the action of the continuous sill in deflecting the flow contributes more to energy dissipation and to jump stability than the shearing and cutting actions of a dentated sill do (Hager 1992; Rand 1967). Considerations about efficiency show that C-jumps and spray jumps usually are considered as ineffective in terms of energy dissipation and are not recommended for stilling basins (Vischer and Hager 1999); A-jumps are usually recommended for easily erodible river beds, whereas less erodible beds can withstand B-jumps and even B_m-jumps.

Drag Force

The correct design of confining appurtenances requires the evaluation of the drag force F_D, which is usually expressed by means of a drag coefficient C_d defined (Hager 1992) as

$$C_d = \frac{F_D}{\frac{1}{2} \cdot \rho \cdot D \cdot B \cdot V_1^2} \tag{3}$$

where V_1 = velocity of supercritical flow before the jump; D = sill height; B = basin width; and ρ = fluid density. For submerged jumps, in Habibzadeh et al. (2011), F_D is directly measured with pressure taps placed on both faces of a baffle sill, and measurements are used to validate the momentum equation, which is then used to predict C_d for baffle blocks. For both submerged and nonsubmerged jumps, in Ohtsu et al. (1991), direct measurements of pressures along the sill provided a relation between C_d and L_s/L_j^* when the flow conditions upstream of the sill are influenced by the downstream depth, and between C_d, F_1, and h_t/h_1 when flow conditions upstream are not influenced by the downstream depth, and for spray jumps.

Pressure Regimes

Along with horizontal forces, that must be correctly estimated to adequately design the confining appurtenances, vertical forces must be evaluated carefully to design slab protection at the bottom of the stilling basin, specifically to avoid uplift or seepage (Fiorotto and Caroni 2014). In a stilling basin, the pressure regime undergoes severe low-frequency fluctuations because of large-scale turbulence structures developing within the basin. Generally, such fluctuations are treated as random variations, so that their analysis concerns probability distribution and statistical parameters such as mean, standard deviation, or RMS, skewness and kurtosis. A statistical parameter usually adopted for pressure analysis is the pressure coefficient C_p^I (Vischer and Hager 1999; Toso and Bowers 1988), which compares pressure RMS or standard deviation, σ with the inflow velocity head

$$C_p^I = \frac{\sigma}{V_1^2/2g} \tag{4}$$

Mean pressure heads P_m, and both negative and positive fluctuations from the mean ΔP^+ and ΔP^-, can be similarly expressed by dimensionless coefficients

$$C_p = \frac{P_m}{V_1^2/2g}; \qquad C_p^{+/-} = \frac{|\Delta P|^{+/-}}{V_1^2/2g} \tag{5}$$

According to a detailed study proposed by Toso and Bowers (1988) concerning unconfined basins, extreme pressure fluctuation depends on the approach Froude number, on the boundary layer development, and on the inflow angle. Also, maximum positive and negative fluctuations take place at different distances from the chute. For basins confined by appurtenances, turbulence is not completely contained within the basin and small fluctuations can be observed downstream (Toso and Bowers 1988).

Experimental Setup

The behavior of the USBR Type II stilling basin was studied by means of an experimental investigation on an acrylic glass model consisting of a detention tank that received the water supply, a filling tank governing the water head above the spillway crest (detention and filling tanks were separated by a filtering wall), and an acrylic glass flume simulating planar flow in the stilling basin and downstream channel. Construction criteria for the structure were followed so that no significant scale effects occurred (Novak et al. 2010; Heller 2011; Pfister and Chanson 2012). The model had a width B equal to 0.85 m, whereas the basin length L_B was equal to 0.75 m. Supercritical flow was generated by a chute (Fig. 1), with an angle of 50° to the horizontal plane. The average sill height D was 0.023 m.

To investigate the influence of the tailwater head-discharge relation, the downstream water head was changed by means of a moving flap. The flume was equipped with eight pressure transducers with an accuracy of ±0.15% and an acquisition frequency of 38.4 Hz, measuring dynamic pressures at the bottom of the basin and of the river in eight measurement points along the center line of the basin, four within and four outside the basin (at a distance of 50, 55, 60, 65, 90, 95, 100, and 105 cm from the terminal section of the chute). A point gage with an accuracy of ±0.5 mm was used to measure water levels and an orifice plate for the monitoring of approach discharge with an accuracy of ±1%.

Experiments were performed for 12 values of the inflow discharge (Table 1). To investigate the influence of the downstream flow on the behavior of the basin, several values of the tailwater level h_t were tested for each discharge value (Table 1 shows maximum and minimum tailwater depths for each tested discharge), whereas the model geometry (namely, basin width and length, and chute slope) were never modified. Table 1 shows that a wider range of Froude numbers was explored than recommended for a USBR Type II stilling basin (Peterka 1984); this was done because

Table 1. Experimental Variables

Q (l/s)	h_0 (m)	h_t maximum (m)	h_t minimum (m)	F_1
4	0.650	0.098	0.046	31.36
10.3	0.667	0.148	0.061	19.89
11.8	0.671	0.157	0.052	18.64
12.9	0.673	0.162	0.053	17.87
14.2	0.676	0.169	0.050	17.07
15.8	0.679	0.176	0.051	16.23
17.8	0.683	0.184	0.052	15.35
19.3	0.685	0.190	0.052	14.78
23	0.691	0.204	0.072	13.61
26.7	0.697	0.216	0.083	12.70
46.1	0.723	0.250	0.129	9.86
65.4	0.743	0.300	0.162	8.41

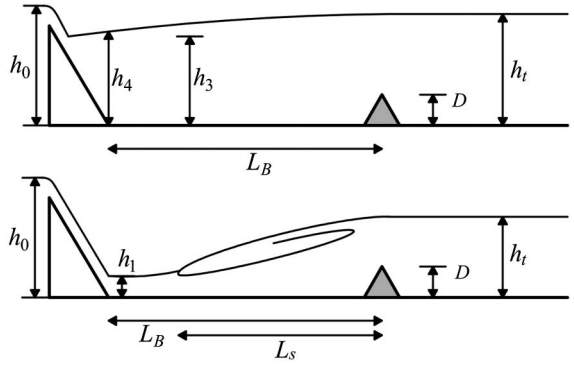

Fig. 3. Experimental variables for submerged (top) and nonsubmerged (bottom) jumps

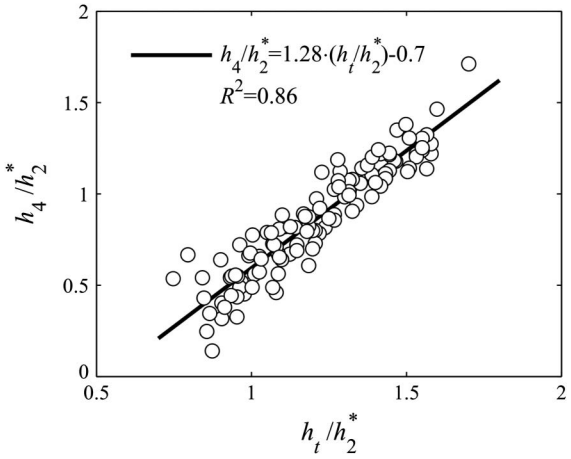

Fig. 4. Correlation among dimensionless inlet depth h_4 and dimensionless tailwater depth h_t

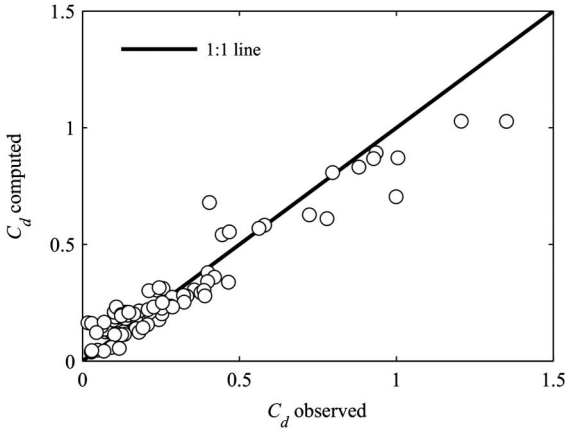

Fig. 5. Correlation among observed and computed C_d

a stilling basin could experience other discharge values than the one used for design purposes. Specifically, a stilling basin usually is designed for a maximum reference discharge; thus, in any other condition the discharge would be lower, in some cases implying an increases in F_1 (Table 1). For this reason, it was important to understand about the hydraulic behavior of such a structure for higher F_1 than design recommendations.

Values of h_1, which are the water depths at the terminal section of the chute (Fig. 3), were computed by means of an energy balance and confirmed by experimental observations for nonsubmerged jumps, and velocity V_1 was computed by means of the continuity law. For submerged jumps, by analogy with hydraulic jumps caused by a sluice gate, V_1 was computed as $\sqrt{2g(h_0 - h_4)}$ (Fig. 3) and h_1 was computed by means of the continuity law. For each test, high-precision pictures were taken and digitalized to obtain instantaneous water profiles for all experimental discharges and tailwater levels (Fecarotta et al. 2016). This allowed systematic information about the distance of jump toe and end from the chute to be obtained, along with water depths h_3 and h_4 at the first wet section and at the terminal section of the chute, respectively.

Discussion

Drag Coefficient

For submerged jumps, the momentum equation was applied between the terminal section of the chute and the terminal section of the jump (Habibzadeh et al. 2011) so that the drag coefficient is

$$C_d = \frac{\left(\frac{h_4}{h_1}\right)^2 - (1+S)^2\left(\frac{h_2^*}{h_1}\right)^2 - 2F_1^2\left\{\left[(1+S)\left(\frac{h_2^*}{h_1}\right)\right]^{-1} - 1\right\}}{\lambda\frac{D}{h_1}F_1^2} \quad (6)$$

where h_4 = water depth at the end section of the chute (h_4/h_1 is called the inlet depth factor); and λ = ratio of blocked width to total width of the basin. Given the particular experienced sill, λ was fixed equal to 1 as if the sill was continuous; this was done in accordance with Hager (1992), stating that the turbulent structure induced by the continuous sill was predominant for the dissipating process over the vortices among the blocks. For the evaluation of h_4, in a submerged jump the water surface can be considered horizontal in most of the calculations; however, as stated by Ohtsu et al. (1991), indirectly computed C_d is very sensitive to errors in the measurements of involved water depths. For practical applications, all terms in Eq. (6) were fixed by the upstream (Q, h_1, h_2^*) and downstream (D, h_t) boundary conditions, whereas h_4 was unknown. However, an empirical relation was found that related h_4/h_2^* and h_t/h_2^* (Fig. 4); the correlation is linear and the regression coefficients were highly similar to the values proposed by Habibzadeh et al. (2011). Fig. 5 shows that, for each test, there was good accordance between the observed C_d [namely C_d obtained with Eq. (6) with proper values of the variables] and the

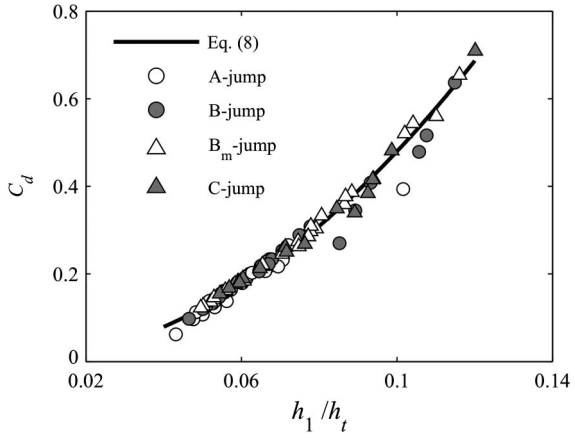

Fig. 6. Drag coefficient for nonsubmerged jumps; interpolating line ($R^2 = 97\%$) is computed for all jump types except for spray jumps

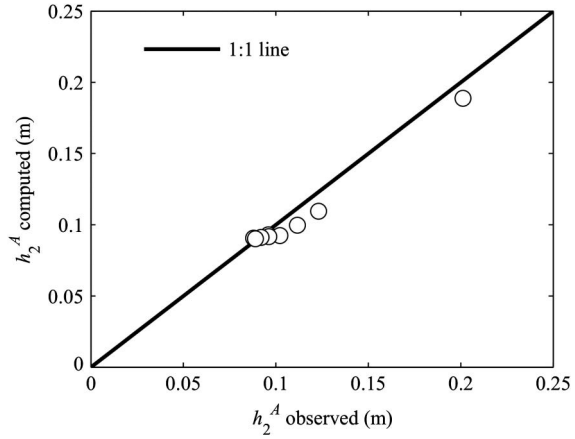

Fig. 7. Comparison between observed and computed depth of incipient submergence h_2^A

computed C_d [namely C_d obtained with Eq. (6) substituting the term h_4/h_1 with the empirical relation proposed in Fig. 4].

For nonsubmerged jumps, C_d can be expressed by Eq. (6) with the inlet factor $h_4/h_1 = 1$. This leads to

$$C_d = \frac{1 - (1+S)^2\left(\frac{h_2^*}{h_1}\right)^2 - 2\mathsf{F}_1^2\left\{\left[(1+S)\left(\frac{h_2^*}{h_1}\right)\right]^{-1} - 1\right\}}{\lambda\frac{D}{h_1}\mathsf{F}_1^2} \quad (7)$$

with all the symbols previously defined. The C_d values computed by means of Eq. (7) with experimental data can be referred to as observed C_d; even if Eq. (7) is available, observed C_d are strictly related to (h_1/h_t) by means of a power function (Fig. 6) consistent with Ohtsu et al. (1991)

$$C_d = 44 \cdot \left(\frac{h_1}{h_t}\right)^2 \quad (8)$$

with coefficient of determination $R^2 = 97\%$. Calibration of regression coefficients in Eq. (8) was performed for all jump types altogether, except for the spray jumps because of the highly turbulent features of such a jump near the dentated sill; spray jumps are treated separately by Ohtsu et al. (1991) as well.

Depth of Incipient Submergence

By substituting Eq. (8) to the left member of Eq. (7) for each incoming discharge (namely h_1 and F_1), it was possible to compute h_t, which was the only unknown variable. This particular tailwater was the depth of incipient submergence h_2^A because only for A-jumps h_1 coincided with the supercritical depth of the hydraulic jump. Fig. 7 proves the accordance of the so computed h_2^A with the experimental observations, namely with the highest experienced tailwater depth giving an A-jump. Consistently with the Belanger relation in Eq. (1), the sequent depth ratio h_2^A/h_1 can be expressed as a linear function of F_1 (Fig. 8); in Fig. 8, the lines corresponding to a constant ratio h_t/h_2^* also are shown, and observed values of h_2^A/h_2^* are interpolated by the line with $h_t/h_2^* = 0.83$

$$\frac{h_2^A}{h_2^*} = 0.83 \Rightarrow \frac{h_2^A}{h_1} = 0.83 \cdot \frac{1}{2} \cdot \left(\sqrt{1 + 8 \cdot \mathsf{F}_1^2} - 1\right) \quad (9)$$

Moreover, in accordance with Peterka (1984), all A-jump experimental data ranged between $h_t/h_2^* = 1$ (that refers to CHJ) and

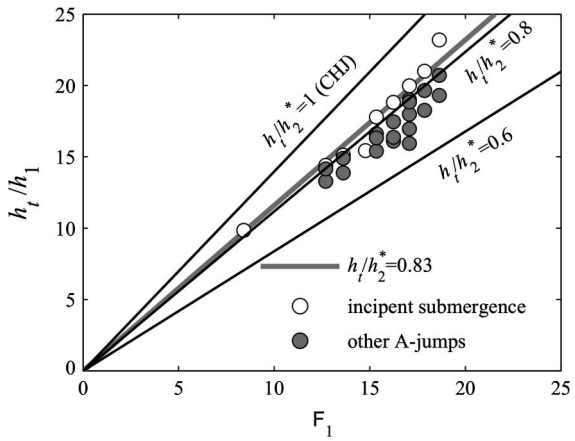

Fig. 8. Correlation between dimensionless sequent depth h_2^A (observed values) and incoming Froude number

$h_t/h_2^* = 0.6$ (Peterka's hydraulic conditions refer to all jump types except for C-jump and spray jumps).

Fig. 8 also shows the sequent depth ratio of CHJ computed with the Belanger relation as a linear function of the Froude number. For a fixed F_1 (consequently fixed h_1), h_2^A was lower than h_2^* in the experimental range of Froude numbers, confirming that for a fixed F_1, an A-jump (namely a forced hydraulic jump completely confined within the basin and with the toe of the jump very close to the terminal section of the chute) occurs for a lower tailwater if compared to a CHJ.

Evaluating h_2^A is highly meaningful when a preliminary distinction between submerged and nonsubmerged conditions is needed. If $h_t < h_2^A$, the jump will be nonsubmerged, moving from A-jump to spray jump with decreasing tailwater; if $h_t > h_2^A$, the jump will be submerged although $h_t < h_2^*$.

Dimensionless Abacus

For nonsubmerged jumps, a dimensionless abacus was built in accordance with Hager and Li (1992) to provide for the identification of jump types and the evaluation of tailwater reduction because of the dentated sill ΔY_s. In particular, in accordance with Hager and Li (1992), ΔY_s was expressed as the sum of two contributions given by L_s/L_j^* and D/h_1, respectively; experimental observations

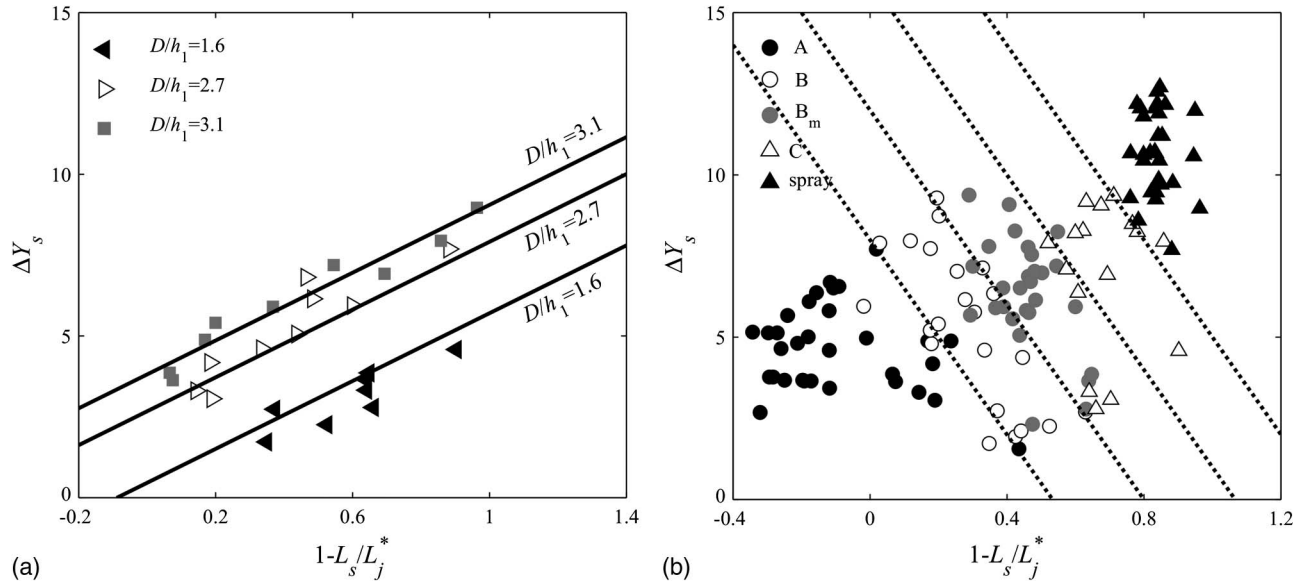

Fig. 9. (a) Relation between $1 - L_s/L_j^*$ and ΔY_s for a selection of experienced D/h_1 values as shown in Eq. (10); (b) dimensionless abacus with distinction among jump types for all experimental data and separation lines according to Eq. (11)

shown in Fig. 9(a) suggested a linear dependence on the former and a square dependence on the latter term

$$\Delta Y_s = 5.2 \cdot \left(1 - \frac{L_s}{L_j^*}\right) + 4.8 \cdot \left(\frac{D}{h_1}\right)^{0.5} - 4.9 \qquad (10)$$

where L_j^* = CHJ length, computed as a simplified function of h_2^* as proposed by Hager (1992). Regression coefficients of Eq. (10) were obtained by minimizing the square sum of errors, namely the differences between ΔY_s computed with Eq. (2), and ΔY_s computed with Eq. (10) for each test (Fig. 10). Eq. (10) shows that for fixed boundary conditions (D, h_1, and h_t), the effect of the sill consists in a tailwater reduction, which is partially given by the sill height and partially by the position of the jump toe. The reduction varied linearly with $1 - L_s/L_j^*$ and the square root of D/h_1, and it was always positive, implying that $h_t \le h_2^A < h_2^*$. Conversely, the abscissa could be positive or negative according to the comparison between L_s and L_j^*; negative values, implying $L_s > L_j^*$ were only experienced for A-jumps with high, D/h_1. However, Eq. (10) differed from results by Hager and Li (1992) in the degree of dependence among variables, because for Hager and Li (1992) ΔY_s depended on $(D/h_1)^{0.7}$ and on the product $(D/h_1)(1 - L_s/L_j^*)^2$.

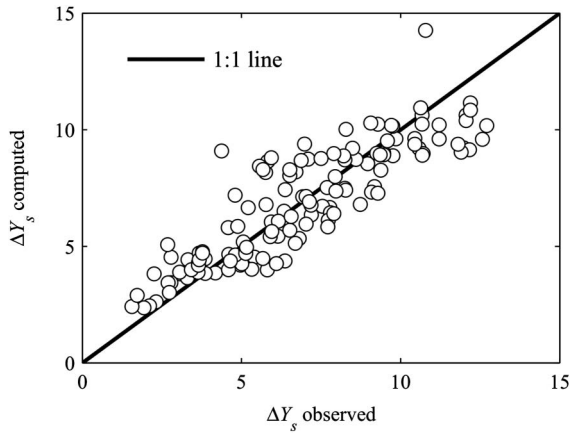

Fig. 10. Accordance between ΔY_s values computed with Eqs. (2) and (10)

Fig. 9(b) shows all experimental data according to their jump type, with separation lines proposed as follows:

$$\Delta Y_s = -15 \cdot \left(1 - \frac{L_s}{L_j^*}\right) + \delta \qquad (11)$$

with intercept δ equal to 8, 12, 16, and 20, marking the passage A/B, B/B_m, B_m/C, and C/spray, respectively. The smallest values of abscissa occurred for A-jumps because the toe of the jump was particularly close to the end of the chute, whereas the opposite happened with spray jumps. For a fixed D/h_1 value, jump types moved from A-jump to spray jump for increasing $1 - L_s/L_j^*$ and ΔY_s.

In practical applications, tailwater reduction is forced by the boundary conditions because the tailwater depth-discharge relation depends on the downstream hydrologic regime. Consequently, for fixed upstream and downstream conditions and a given sill height, Eq. (10) and Fig. 9 allow for L_s and jump type to be estimated.

Dissipation Efficiency

Dissipation efficiency ε_t for submerged jumps was computed in accordance with Habibzadeh et al. (2011) as the difference between energy heads before (E_0) and after the jump (E_t), normalized to E_0

$$\varepsilon_t = \frac{E_0 - E_t}{E_0} = \frac{\left(h_4 + \frac{V_t^2}{2g}\right) - \left(h_t + \frac{V_t^2}{2g}\right)}{\left(h_4 + \frac{V_t^2}{2g}\right)} \qquad (12)$$

where V_t = flow velocity corresponding to tailwater depth h_t. Fig. 11 shows ε_t as a function of submergence factor S for different F_1 values. For submerged jumps, in perfect accordance with Habibzadeh et al. (2011) (although the experienced Froude numbers are significantly higher), for fixed F_1, starting from maximum submergence, dissipation efficiency linearly increased with decreasing S. The maximum efficiency $\varepsilon_{t\max}$ of submerged jumps

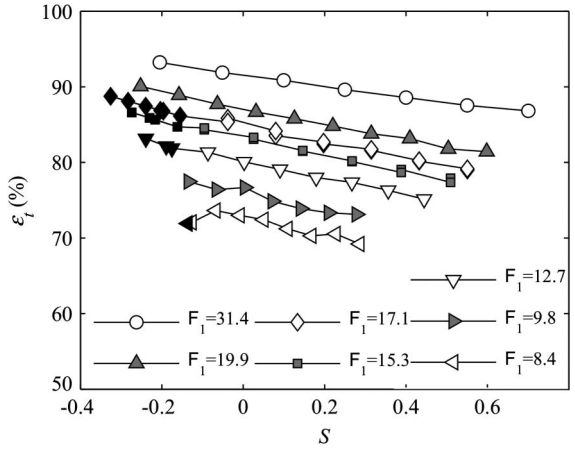

Fig. 11. Dissipation efficiency as a function of submergence factor for A-jumps (white and grey marks) and submerged jumps (black marks)

was always experienced for negative submergence factors and it increased with increasing F_1.

As concerns nonsubmerged jumps, efficiency of A-jumps was computed by means of Eq. (12) with $h_4 = h_1$. Fig. 11 shows that A-jump efficiencies also decreased with increasing S, with almost the same linear trend as the submerged jumps. For the highest F_1, ε_t can be considered a unique decreasing function of S for both jump types, whereas for the lowest F_1, a slight decrease in efficiency was observed in accordance with Habibzadeh et al. (2011). Consequently, the maximum efficiency $\varepsilon_{t\max}$ of A-jumps was higher than $\varepsilon_{t\max}$ for submerged jumps in all cases, except for the lowest F_1.

For submerged and A-jumps, Fig. 12 shows $\varepsilon_{t\max}$ as a function of F_1 along with ε_2^* (computed energy heads corresponding to h_1 and h_2^*), which is also a function of F_1. The comparison shows that in the optimal conditions (conditions that give the maximum experienced energy loss for each F_1), the dissipation efficiency for a USBR Type II stilling basin with submerged jump is higher than that of a free jump, and it is roughly similar to the energy loss given by a basin with baffle blocks (Habibzadeh et al. 2011). In turn, dissipation efficiency of submerged jumps is lower than the efficiency of a USBR Type II stilling basin with an A-jump, which was the highest possible for the examined conditions.

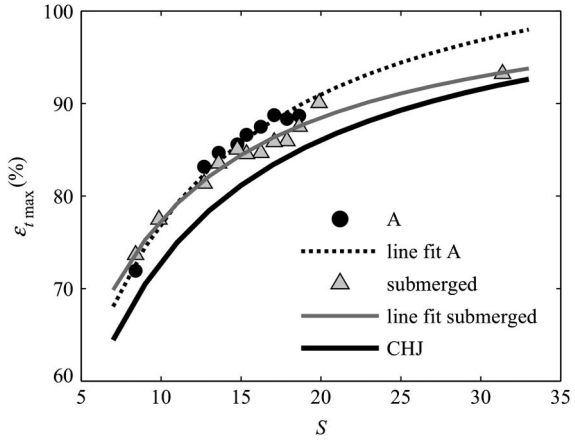

Fig. 12. Maximum dissipation efficiency for submerged and A-jumps in USBR Type II basin and in classical hydraulic jump

Pressure Regime

Pressure measurements, especially pressure fluctuations, can give additional information to the dissipation efficiency of a stilling basin because they are related to the remaining turbulence downstream of the confining appurtenance. The trends of mean pressure heads roughly reproduce the water surface profile and the dissipation vortex for nonsubmerged jumps; therefore, pressures outside the basin are particularly higher than inside pressures for spray jumps because of the larger water depth differences. In Fecarotta et al. (2016), pressure coefficients C_p^I, measuring the standard deviation of fluctuations, were shown to significantly decrease downstream of the dentated sill, showing that most of the turbulence was included within the stilling basin for all the jump types except for the spray jump. Moreover, according to Fecarotta et al. (2016), C_p^I had a peak outside of the basin only for spray jumps, demonstrating how this jump type is inefficient in dissipating energy, whereas the peak was located inside the basin for all the other jump types. The lowest values of fluctuation magnitude occurred downstream of the sill for all jump types, except for spray jump. Also, for submerged, A- and B-jumps, the extreme C_p^- was higher than the extreme C_p^+ in accordance with Toso and Bowers (1988), whose study concerned an unconfined stilling basin.

In Fig. 13, $C_{p\max}^-$ and $C_{p\max}^+$, namely the maximum measured values of C_p^- and C_p^+ for each experimental configuration, are shown as a function of h_t/h_1, along with power functions that can be used to successfully predict extreme fluctuations; coefficients of determination were equal to 62 and 71%, respectively

$$C_{p\max}^- = 12.8 \cdot \left(\frac{h_t}{h_1}\right)^{-1.3} \tag{13}$$

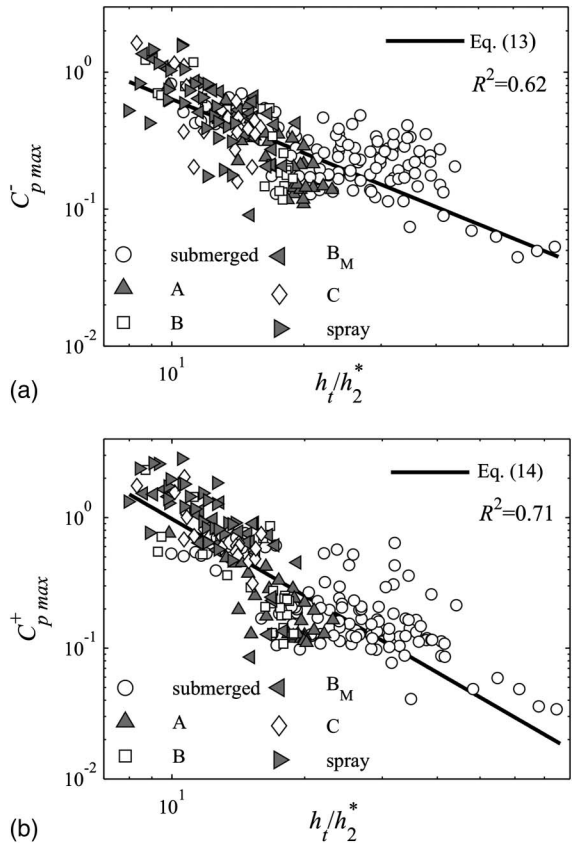

Fig. 13. Magnitude of (a) extreme negative and (b) positive fluctuations from the mean as a function of h_t/h_2^*

$$C^{+}_{p\max} = 87.3 \cdot \left(\frac{h_t}{h_1}\right)^{-2} \quad (14)$$

In both cases, maximum and minimum values of abscissa were attained by submerged and spray jumps, respectively; however, for submerged jumps, pressure coefficients were similar, roughly lower than 0.5, whereas moving to C-jump and spray jumps, $C^{+}_{p\max}$ was significantly higher than $C^{-}_{p\max}$. This constitutes an additional reason that hinders the adoption of a C-jump or spray jump within a stilling basin. The use of a power function was in accordance with Toso and Bowers (1988).

Conclusions

An experimental campaign was undertaken on an USBR Type II stilling basin to understand its hydraulic behavior and dissipation efficiency. Experiments covered a wider Froude range than design recommendations given that stilling basins can experience different working conditions, whose hydraulic consequences should be understood. As concerns the first issue, six jump types were found possible, namely submerged jumps and jump types from A-jump to spray according to the classification by Hager and Li (1992). A dimensionless representation of results was obtained by means of the variables proposed by Hager and Li (1992), correlating tailwater reduction because of the sill ΔY_s to the dimensionless jump toe-sill distance and dimensionless sill height. Such an abacus provides for the jump type and position once upstream and downstream hydraulic conditions are fixed. As concerns dissipation efficiency, analyses were undertaken in accordance with Habibzadeh et al. (2011). Correlation of energy losses to the submergence factor showed that dissipation efficiency increases with decreasing submergence, so that A-jumps are more efficient than submerged jumps, which, in turn, are more efficient than classical hydraulic jumps in unconfined basins. An in-depth look at pressure fluctuations showed that high submergence factors (namely submerged and A-jumps) are characterized by the smallest pressure fluctuations. All considered, A-jumps proved to be the most efficient jump type for USBR Type II stilling basins.

Experimental results provided for the design criteria of an USBR Type II stilling basin. Given a design discharge and Froude number, Eq. (9) enables estimation of the depth of incipient submergence. If a tailwater is fixed, it is possible to know whether a submerged ($h_t > h_2^A$) or a nonsubmerged ($h_t < h_2^A$) jump will occur, and to know what is the value of the tailwater reduction because of the sill ΔY_s in the latter case. Then, by means of Eq. (10), if sill height is known, the abacus provides for the jump position L_s and jump type (Fig. 9), whereas if the sill must be dimensioned, fixing a jump type and position enables estimation of D. When designing the sill, given the suggestions by Peterka (1984), the drag force (namely the drag coefficient) must be evaluated by means of Eq. (6) if the jump is submerged (with estimated correlation between h_4 and h_t), or with Eq. (8) if the jump is not submerged. Dissipation efficiency is provided by Eq. (12) (with $h_4 = h_1$ if the jump was not submerged). Once the hydraulic conditions have been determined, it is possible to estimate pressure extreme fluctuations on the protection slab at the bottom of the basin by means of Eqs. (13) and (14), whereas the average pressure head coincides with the surface profile.

Acknowledgments

The laboratory equipment used for the experimental campaign was financed by Studio Ing. Pietrangeli s.r.l. (Rome, Italy).

Notation

The following symbols are used in this paper:

B = basin width (m);
C_d = drag coefficient (-);
C'_p = standard deviation pressure coefficient = $\sigma/(V_1^2/2g)$;
C^{-}_p = extreme negative fluctuation pressure coefficient = $|\Delta P^{-}| \cdot V_1^{-2} \cdot 2g$;
C^{+}_p = extreme positive fluctuation pressure coefficient = $|\Delta P^{+}| \cdot V_1^{-2} \cdot 2g$;
D = sill height (m);
E = energy head (m);
F_1 = incoming Froude number;
F_D = drag force (N);
g = gravity acceleration ($m \cdot s^{-2}$);
h = water depth (m);
L_B = basin length (m);
L_j = jump length (m);
L_s = jump toe/sill distance (m);
P = pressure head (m);
Q = discharge ($m^3 \cdot s^{-1}$);
S = submergence factor (-);
V = flow velocity ($m \cdot s^{-1}$);
x_p = distance between terminal section of the chute and jump toe (m);
ΔY_s = tailwater reduction because of the sill (-);
δ = intercept for jump types separation lines (-);
λ = blocks/basin width ratio (-);
ε = dissipation efficiency (%);
ρ = fluid density ($kg \cdot m^3$); and
σ = pressure head standard deviation (m).

Subscripts

0 = section upstream of the chute;
1 = terminal section of the chute (supercritical flow);
2 = subcritical sequent depth;
3 = first wet section of the chute;
4 = terminal section of the chute (submerged flow);
m = mean value;
max = maximum value; and
t = tailwater depth.

Superscripts

* = classical hydraulic jump; and
A = A-jump.

References

Alikhani, A., Behrozi-Rad, R., and Fathi-Moghadam, M. (2010). "Hydraulic jump in stilling basin with vertical end sill." *Int. J. Phys. Sci.*, 5(1), 25–29.

Bradley, J. N., and Peterka, A. J. (1957). "The hydraulic design of stilling basins: Hydraulic jumps on a horizontal apron (basin I)." *J. Hydr. Eng. Div.*, 83(5), 1–32.

Chanson, H. (2015). *Energy dissipation in hydraulic structures*, CRC Press, Leiden, Netherlands.

Chow, V. T. (1959). *Open channel hydraulics*, McGraw-Hill, New York.

Fecarotta, O., Carravetta, A., Del Giudice, G., Padulano, R., Pontillo, M., and Brasca, A. (2016). "Experimental results on the physical model of an USBR type II stilling basin." *Proc., Riverflow 2016—8th Int.*

Conf. on Fluvial Hydraulics, CRC Press/Balkema, Leiden, Netherlands.
Fiala, G. R., and Albertson, M. L. (1961). "Manifold stilling basin." *J. Hydr. Eng. Div.*, 87(4), 55–81.
Fiorotto, V., and Caroni, E. (2014). "Unsteady seepage applied to lining design in stilling basins." *J. Hydraul. Eng.*, 10.1061/(ASCE)HY.1943-7900.0000867, 04014025.
Flammer, G. H., Skogerboe, G. V., Wei, C. Y., and Rasheed, H. (1970). "Closed conduit to open channel stilling basin." *J. Irrig. Drain. E.*, 96(1), 1–10.
Govinda Rao, N. S., and Rajaratnam, N. (1963). "The submerged hydraulic jump." *J. Hydraul. Eng. Div.*, 89(1), 139–162.
Habibzadeh, A., Wu, S., Ade, F., Rajaratnam, N., and Loewen, M. R. (2011). "Exploratory study of submerged hydraulic jumps with blocks." *J. Hydraul. Eng.*, 10.1061/(ASCE)HY.1943-7900.0000347, 706–710.
Hager, W. H. (1992). *Energy dissipators and hydraulic jump*, Kluwer, London.
Hager, W. H., and Li, D. (1992). "Sill-controlled energy dissipator." *J. Hydraul. Res.*, 30(2), 165–181.
Heller, V. (2011). "Scale effects in physical hydraulic engineering models." *J. Hydraul. Res.*, 49(3), 293–306.
Keim, S. R. (1962). "The Contra Costa energy dissipator." *J. Hydraul. Eng. Div.*, 88(2), 109–122.
Novak, P., Guinot, V., Jeffrey, A., and Reeve, D. E. (2010). *Hydraulic modeling: An introduction*, Spon Press, London.
Ohtsu, I., Yasuda, Y., and Yamanaka, Y. (1991). "Drag on vertical sill of forced jump." *J. Hydraul. Res.*, 29(1), 29–47.
Peterka, A. J. (1984). "Hydraulic design of stilling basins and energy dissipators." U.S. Dept. of the Interior, Bureau of Reclamation, Denver.
Pfister, M., and Chanson, H. (2012). "Discussion of "Scale effects in physical hydraulic engineering models" by Valentin Heller." *J. Hydraul. Res.*, 50(2), 244–246.
Rand, W. (1967). "Efficiency and stability of forced hydraulic jump." *J. Hydraul. Eng. Div.*, 93(4), 117–127.
Tiwari, H. L., and Goel, A. (2014). "Effect of end sill in the performance of stilling basin models." *Am. J. Civ. Eng. Archit.*, 2(2), 60–63.
Tiwari, H. L., Goel, A., and Gahlot, V. K. (2011). "Experimental study of sill controlled stilling basins for pipe outlet." *Int. J. Civ. Eng. Res.*, 2(2), 107–117.
Toso, J. W., and Bowers, C. E. (1988). "Extreme pressures in hydraulic-jump stilling basins." *J. Hydraul. Eng.*, 10.1061/(ASCE)0733-9429(1988)114:8(829), 829–843.
Verma, D. V. S., and Goel, A. (2000). "Stilling basins for pipe outlets using wedge-shaped splitter block." *J. Irrig. Drain. Eng.*, 10.1061/(ASCE)0733-9437(2000)126:3(179), 179–184.
Vischer, D. L., and Hager, W. H. (1999). *Dam hydraulics*, Wiley, Chichester, U.K.
Vollmer, E., and Khader, M. H. A. (1971). "Counter current energy dissipator for conduit outlets." *Int. J. Water Power*, 23(7), 260–263.